# Interfacial Interaction in Organic-Inorganic Heterostructure via W-N bond for Enhanced Photocatalytic $H_2$ Production

Rui Ma,[a,b] Juan Li,[a,b] Yao Wang,[a,b] Xu-Bing Li,*[a,b] Chen-Ho Tung,[a,b] and Li-Zhu Wu[a,b]

a. Key Laboratory of Supramolecular Photochemistry&CAS-HKU Joint Laboratory on New Materials, New Cornerstone Science Laboratory, Technical Institute of Physics and Chemistry, Chinese Academy of Sciences, Beijing 100190, China.

b. School of Future Technology, University of Chinese Academy of Sciences, Beijing 100049, China.

# Table of Contents

| | |
|---|---|
| **Section A** | **General Methods and Materials** |
| **Section B** | **Synthetic Procedures** |
| **Section C** | **Characteristic** |
| **Section D** | **Photocatalysis experiment** |
| **Section E** | **Figure S1-S16 and Table S1-2** |
| **Section F** | **Reference** |

## Section A General Methods and Materials

Chemicals: $Na_2WO_4 \cdot 2H_2O$, $HNO_3$, $CoSO_4$, $K_3[Fe(CN)_6]$, $HAuCl_4$, $Cu(NO_3)_2 \cdot 3H_2O$ and $NaIO_3$ were purchased from Beijing Innnochem Technology Co., Ltd. 2,5-diaminobenzene-1,4-dithiol dihydrochloride, Yttrium (III) trifluoromethanesulfonate, triethyl orthoacetate, 1,3,5-benzenetricarboxaldehyde (BTCA) and benzoic anhydride were purchased from Shanghai Aladdin Bio-Chem Technology Co., LTD. All the common solvents were purchased from Shanghai Aladdin Bio-Chem Technology Co., LTD and used as received without further purification.

## Section B Synthetic Procedures

### Synthesis of $WO_3$ nanosheets:

Add 5 mL of nitric acid solution to 25 mL of ultrapure water and stir for 10 minutes. Meanwhile, disperse 0.494 g of sodium tungstate dihydrate ($Na_2WO_4 \cdot 2H_2O$) in 5 mL of ultrapure water. Then, slowly add the $Na_2WO_4$ solution to the $HNO_3$ solution. Stir at room temperature for 30 minutes to ensure thorough mixing. Transfer the mixture to a 50 mL Teflon-lined autoclave and maintain at 180 °C for 3 hours. After cooling to room temperature, centrifuge the yellow product and wash it with ultrapure water and ethanol. Finally, vacuum dry at 60 °C for 6 hours to obtain $WO_3$ nanosheets.

### Loading of the cocatalyst:

(1) Preparation of $FeCoO_x$-$WO_3$. It is prepared by in-situ photo-deposition method. Pure water solution containing calculated amounts of $CoSO_4$ and $[Fe(CN)_6]^{3-}$ ions is used for the synthesis of $FeCoO_x$-$WO_3$, and 0.5 mmol $NaIO_3$ is added as an electron scavenger. The loading amounts of Fe and Co were 2.5 wt% respectively.

(2) Preparation of $FeCoO_x$-$WO_3$-Au. Au nanoparticles are deposited on the surface of $FeCoO_x$-$WO_3$ by photo-deposition method. Generally, 150 mg of $FeCoO_x$-$WO_3$ powder was dispersed in deionized water containing calculated amounts of $HAuCl_4$ (Au loading amount is 3.0 wt%). Then it is illuminated with a 400 nm LED for 2 hours. The obtained powder after filtration and washing is denoted as 5 wt%$FeCoO_x$-$WO_3$-3 wt% Au accordingly.

(3) Preparation of Cu-$WO_3$-Au. Cu is loaded onto $WO_3$ through an easy impregnation method (Cu-$WO_3$). A certain amount of $Cu(NO_3)_2 \cdot 3H_2O$ is dissolved in 0.5 mL of deionized water and continuously stirred (600 rpm). It is then dropped into 0.5 g of $WO_3$ nanoparticles. The mixture is then dried under stirring at 500 rpm at 60 °C. After evaporating all the water, the solid is transferred to an aluminum oxide crucible with a cover and calcined in an air atmosphere in a muffle furnace at 400 °C for 2 hours. After cooling naturally to room temperature in the furnace, the obtained sample is rinsed with water three times. Subsequently, 3 wt% Au nanoparticles are loaded onto Cu-$WO_3$ by the photo deposition method.

### Synthesis of 2,6-dimethy [1,3] thiazolo[5,4-f] [1,3] benzothiazole (DTBT):

2,5-diaminobenzene-1,4-dithiol dihydrochloride (0.687 g 2.8 mmol), Yttrium (III) trifluoromethanesulfonate (0.092 g, 0.17 mmol), triethyl orthoacetate (5 mL, 27.3 mmol), N, N-dimethylacetamide (5 mL) and pyridine (0.55 mL) are heated at 80 °C for 3 hours. After cooling to room temperature, the solution was poured into 100 mL water and extracted with 200 mL dichloromethane. The organic solution was dried, and the solvent was evaporated under vacuum to yield an off-white powder (0.28 g, 45%). $^1$H NMR (400 MHz, $CDCl_3$): δ 2.87 (6 H, s), 8.36 (2 H, s).

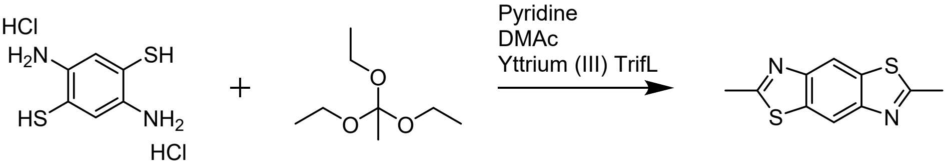

## Synthesis of 2D c-COFs:

A Pyrex tube (d=10 mm) was charged with 1,3,5-benzenetricarboxaldehyde (BTCA, 15 mg, 0.093 mmol), 2,6-dimethy [1,3] thiazolo [5,4-f] [1,3] benzothiazole (DTBT, 30.6 mg, 0.138 mmol), and benzoic anhydride (62.78 mg, 0.276 mmol). The tube was flash frozen at 77 K (liquid $N_2$ bath), evacuated for 15 mins, and flame sealed. The reaction was carried out at 200 °C for 5 days to give a yellow solid. The yellow solid was washed with tetrahydrofuran (THF), acetone, and methanol. Finally, the material was dried at 120 °C under vacuum condition to yield 2D c-COFs.

## In-situ growth of COFs films on the $WO_3$ surface:

1,3,5-benzenetricarboxylic acid (BTCA), 2,6-dimethyl [1,3] thiazole[5,4-f] [1,3] benzothiazole (DTBT), benzoic anhydride, and 5 wt% $FeCoO_x$-$WO_3$-3 wt% Au (the mass ratio of COFs monomer to $WO_3$ is 0.5:10) were added into a Pyrex tube (d = 10 mm). The tube was rapidly frozen under a liquid $N_2$ bath at 77 K, vacuumed for 15 minutes, and sealed with a flame. The reaction was carried out at 200 °C for 5 days, resulting in a yellow solid. The yellow solid was washed with tetrahydrofuran (THF), acetone, and methanol. Finally, it was dried under vacuum at 120 °C to obtain 5 wt% 2D c-COFs/$WO_3$. Heterogeneous structures of 3 wt%, 5 wt%, 7 wt%, 10 wt% and 20 wt% 2D c-COFs/$WO_3$ were synthesized respectively based on different mass ratios of the COFs monomer to $WO_3$.

## Section C Characteristic

### C-1 Solution state nuclear magnetic resonance

$^1$HNMR spectra were collected on a Bruker AVANCE 400 III WB spectrometer.

### C-2 Solid state nuclear magnetic resonance

$^{13}$C cross polarization/magic angle spinning solid state nuclear magnetic resonance (CP/MAS NMR) experiments were performed on a Bruker AVANCE 400 WB spectrometer operating at 100.62 MHz for $^{13}$C using a double resonance 4 mm MAS NMR probe and a sample spinning rate of 10 kHz. The cross-polarization time was 1 ms.

### C-3 Fourier-Transform infrared spectroscopy (FT-IR)

Fourier-Transform Infrared (FT-IR) spectra were recorded on Excalibur 3100.

### C-4 Small Angle X-ray Scattering (SAXS)

Small Angle X-ray Scattering (SAXS) measurements were carried out using a Nano inXider.

### C-5 UV-vis absorption spectra (UV-vis)

UV-vis absorption spectra were measured on an Agilent Cary 7000 at room temperature in an integration sphere.

### C-6 Scanning electron microscopy (SEM)

Morphological analysis of the 2D c-COFs and x wt% 2Dc-COFs/$WO_3$ were performed using on a field emission scanning electron microscope HITACHI S-4800 field emission scanning electron microscope. Powder samples were placed over sample stage and imaged under high vacuum.

### C-7 Transmission electron microscopy (TEM)

Transmission electron microscope (TEM) characterizations were conducted using JEM-2100 with an accelerating voltage of 200 KV.

### C-8 Energy dispersive spectrogram (EDS)

Energy dispersive spectrogram (EDS) maps were recorded on an aberration-corrected JEM-ARM300F operated at 300 kV.

### C-9 The photoluminescence (PL)

The photoluminescence (PL) tests were recorded on a HoribaFluoremax-4 PLUS spectrofluorometer (HORlBA Instruments Incorporated, EdisonUSA) with a xenon lamp as an excitation light source.

### C-10 The Time-resolved photoluminescence (TRPL)

The time-resolved photoluminescence (TRPL) tests were recorded on a LP-920 (Edinburgh Instruments) using a 405 nm laser.

### C-11 The X-ray photoelectron spectroscopy (XPS)

The X-ray photoelectron spectroscopy (XPS) was recorded on a ESCALAB 250Xi with Al-Kα radiation.

### C-12 Femtosecond transient absorption spectroscopy (fs-TA)

The femtosecond transient absorption spectroscopy (fs-TA) was recorded on a Helios pump-probe system (Ultrafast Systems LLC) coupled with an amplified femtosecond laser system (Coherent, 35 fs, 1kHz, 800 nm).

### C-13 Raman spectrum

The Raman spectrum was recorded on a Renishaw inVia-Qontor using a 325 nm wavelength laser.

### C-14 Electrochemical measurements

Electronic properties experiments, such as photoelectric current measurement (i-t) and electrochemical impedance spectroscopy (EIS), were measured on a CHI 660E in a three-electrode electrochemical cell equipped with a salt bridge. The scan rate was 0.1 V $s^{-1}$. The reference electrode was based on the Ag/AgCl couple. The working electrode was a catalyst-modified FTO working electrode and was cleaned by sonication in ethanol for 15 min. The sample (5 mg) was dispersed in ethanol (0.5 mL) and ethylene glycol (0.5 mL) by sonication to get a slurry. The slurry was spread onto pretreated FTO glass (1mg catalyst sample in 1 $cm^2$ FTO electrode). The electrolyte was a 0.1 M $Na_2SO_4$ aqueous solution (pH 6.8) and purged with nitrogen gas for 0.5 h before the experiments. The visible light was generated by a 300W Xe lamp (CEL-S500/350). The EIS data was obtained by testing the open-circuit voltage (OCV) of each sample.

### C-15 AQY calculation

$$\mathrm{AQY} = \frac{2 \times \mathrm{n(H2)} \times \mathrm{NA}}{\mathrm{Nincident\ -\ photon}} \times 100\%$$

$$\mathrm{E0} = \frac{\mathrm{hc}}{\lambda} = \frac{6.626 \times 10 - 34 \times 3 \times 108}{415 \times 10 - 9} = 4.79 \times 10 - 19\ \mathrm{J}$$

$$\mathrm{N} = \frac{\mathrm{E}}{\mathrm{E0}} = \frac{80 \times 6 \times 10 - 3 \times 3600}{4.79 \times 10 - 19} = 3.6 \times 1021$$

$$\mathrm{AQY} = \frac{2 \times 147 \times 10 - 6 \times 6.02 \times 1023}{3.6 \times 1021} \times 100\% = 4.92\ \%$$

## Section D Photocatalysis experiment

**Photocatalytic hydrogen production experiment:** Add 2 mg of photocatalyst into a 15 mL heat-resistant glass tube, use 5 mL of pure water as the solvent, ultrasonicate for 30 minutes, then add 0.5 mmol of Vc as the electron sacrificial agent, 1 μL of 8 wt% chloroplatinic acid solution as the cocatalyst. Remove the air with Ar gas for 30 minutes, then introduce a certain amount of methane as the standard gas, seal with wax and place it in a 415 nm LED for 2 hours of illumination. Use Shimadzu Nexis GC-2030 to test the hydrogen production data.

## Section E Figure S1-S16

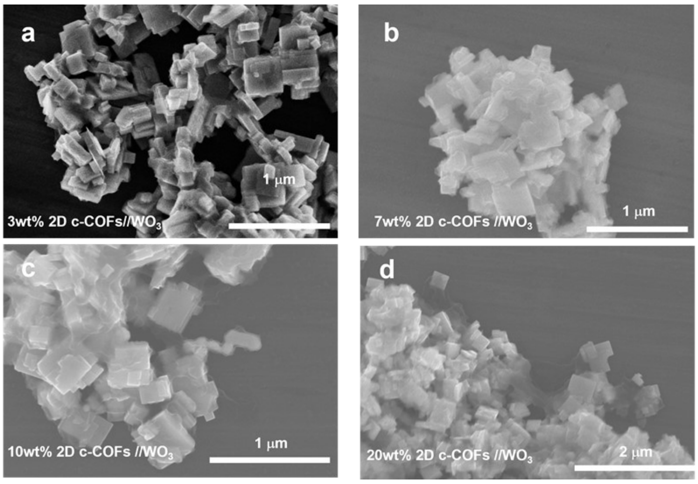

Fig. S1 The SEM images of 3 wt%, 7 wt%, 10 wt% and 20 wt% 2D c-COFs/$WO_3$.

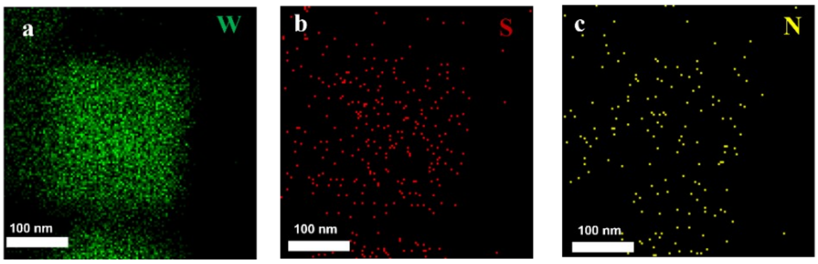

Fig. S2 The EDS mapping images of 5 wt% 2D c-COFs/$WO_3$.

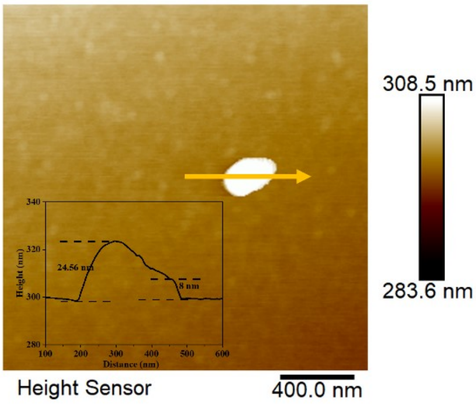

Fig. S3 The AFM images of 5 wt% 2D c-COFs/$WO_3$.

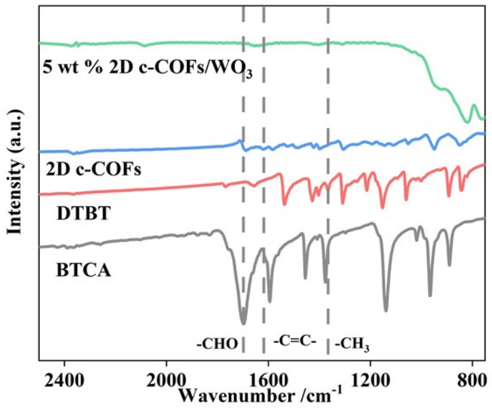

Fig. S4 The Fourier transform infrared spectra of 5 wt% 2D c-COFs/WO$_3$, 2D c-COFs, DTBT and BTCA.

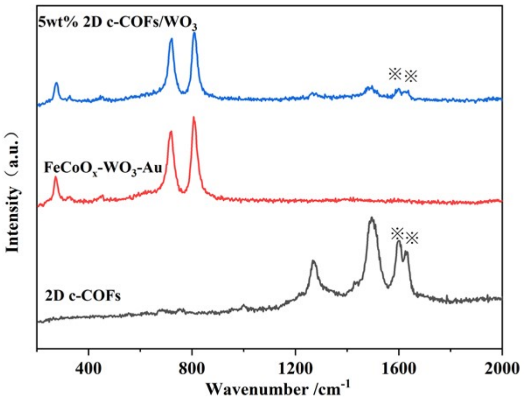

Fig. S5 Raman spectrum of FeCoO$_x$-WO$_3$-Au, 2D c-COFs and 5 wt% 2D c-COFs/WO$_3$.

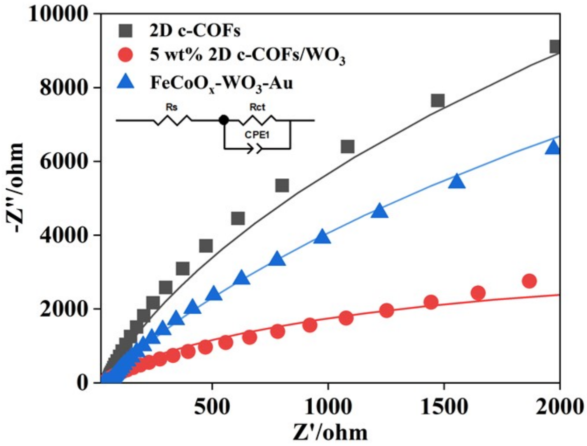

Fig. S6 The EIS of FeCoO$_x$-WO$_3$-Au, 2D c-COFs and 5 wt% 2D c-COFs/WO$_3$.

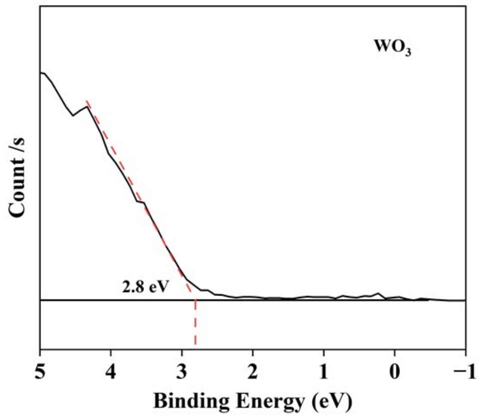

Fig. S7 The XPS valence band spectrum of WO$_3$.

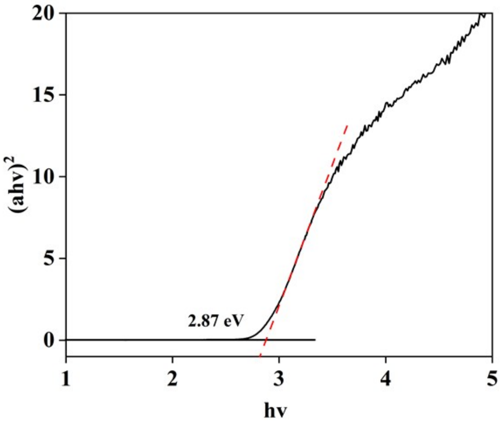

Fig. S8 The *Tauc* curve of WO$_3$.

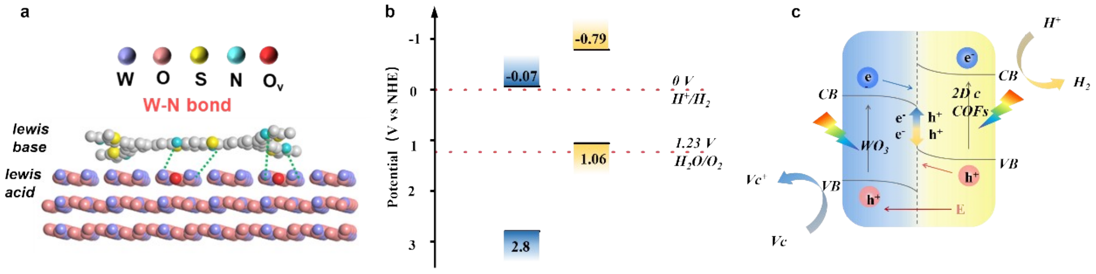

Fig. S9 The interface structure (a), band structure (b) and schematic diagram of the charge transfer mechanism (c) at the 2D c-COFs/WO$_3$ heterostructure. The color balls: purple, W; pink, O; yellow, S; blue, N; red, O$_V$.

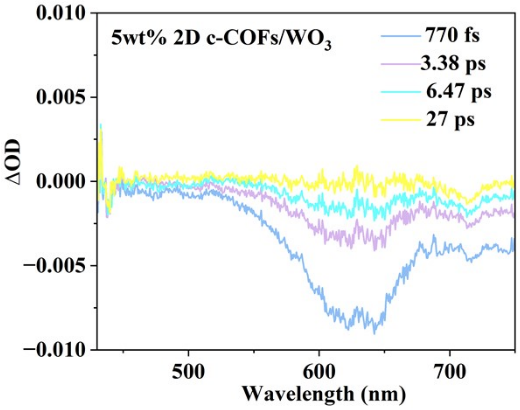

Fig. S10 The fs-TA spectra of the 5 wt% 2D c-COFs/WO$_3$.

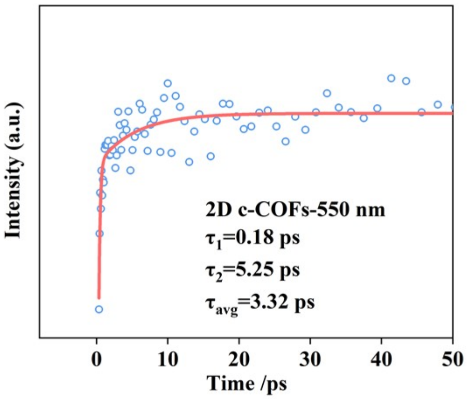

Fig. S11 The double-exponential fitting curves of the photogenerated carrier dynamics of pristine 2D c-COFs.

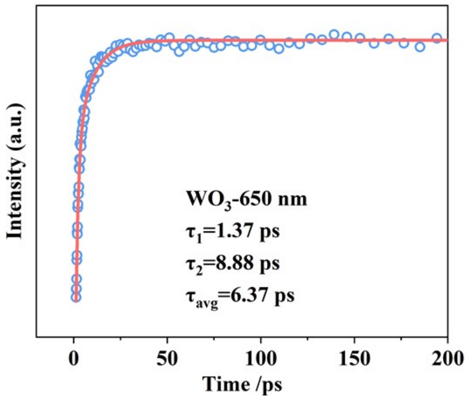

Fig. S12 the double-exponential fitting curves of the photogenerated carrier dynamics of WO$_3$.

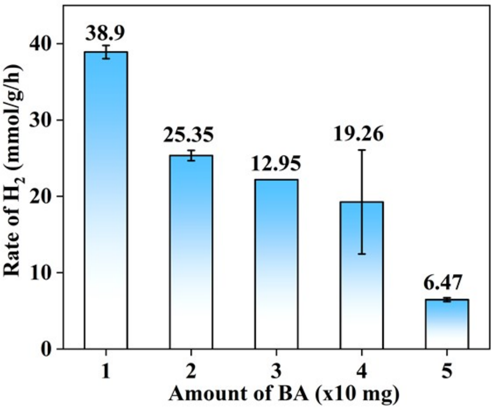

Fig. S13 BA addition amount screening experiment.

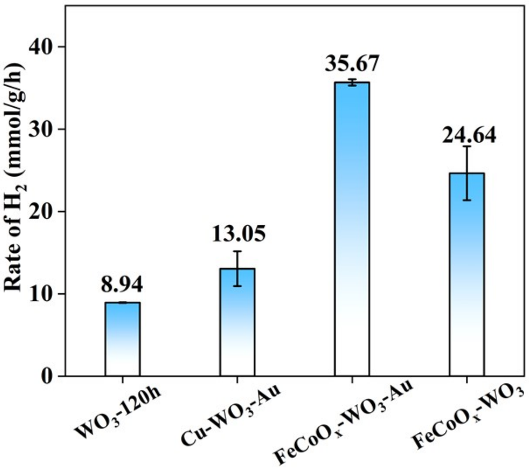

Fig. S14 Screening experiment of cocatalyst on $WO_3$ substrate.

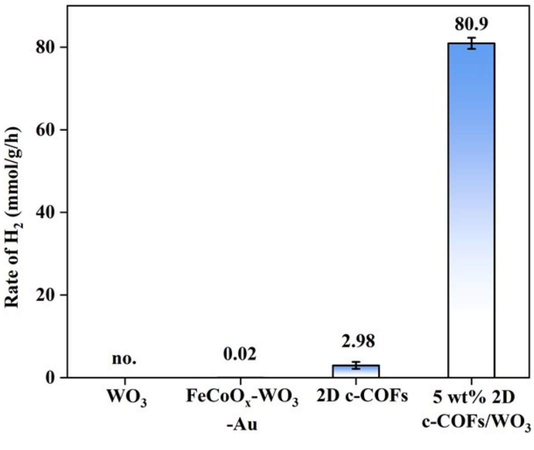

Fig. S15 Comparison of photocatalytic hydrogen production rates of $WO_3$, $FeCoO_x$-$WO_3$-Au, 2D c-COFs and 5 wt% 2D c-COFs/$WO_3$ under the same conditions.

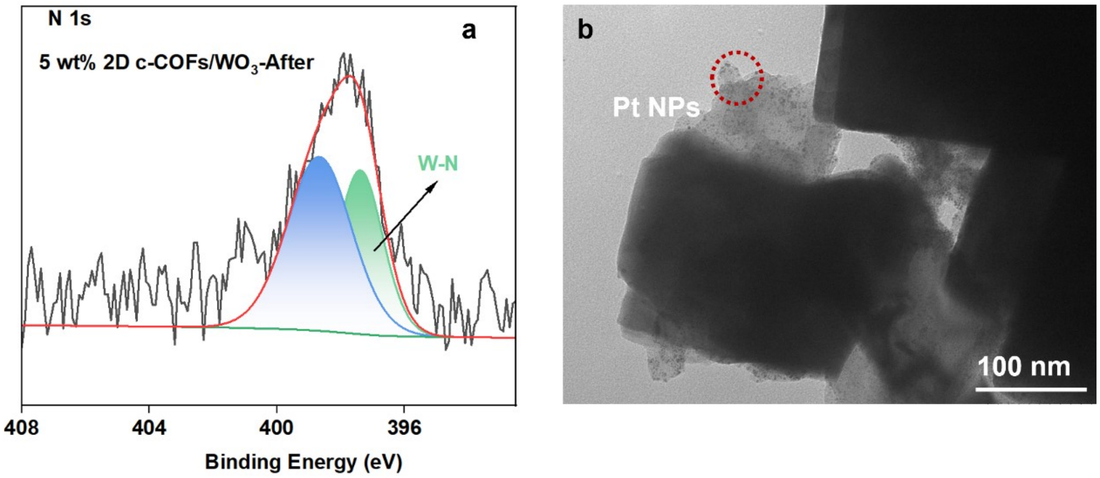

Fig. S16 The N 1s XPS spectrum (a) and the TEM image (b) of 5 wt% 2D c-COFs/$WO_3$ after photocatalytic reaction.

Table S1. The fitted values of $R_s$ and $R_{ct}$ of $FeCoO_x$-$WO_3$-Au, 2D c-COFs and 5 wt% 2D c-COFs/$WO_3$.

| sample | $R_s$ (Ω) | $R_{ct}$ (kΩ) |
|---|---|---|
| 2D c-COFs | 44.03 | 73.5 |
| $FeCoO_x$-$WO_3$-Au | 48.01 | 54.9 |
| 5 wt% 2D c-COFs/$WO_3$ | 31.56 | 6.55 |

Table S2. Comparison of photocatalytic hydrogen production rates of 5wt% 2D c-COFs/$WO_3$ with other organic/inorganic heterojunction photocatalysts.

| Sample | Light | Rate(mmol/g/h) | sacrificial agent | Ref. |
|---|---|---|---|---|
| $S_v$-ZIS/TpPa-1 | 300 W Xe<br>(λ>420 nm) | 2.75 ($H_2$) | Vc | 1[1] |
| FS-COF/$WO_3$ | 300 W Xe<br>(λ>420 nm) | 24.7 | Vc | 2[2] |
| CZS-FOCTF | 350 W Xe<br>(λ>420 nm) | 247.62 ($H_2$) | $Na_2S$/$Na_2SO_3$ | 3[3] |
| HCPDI@ZIS | 300 W Xe<br>(λ>400 nm) | 0.275 ($H_2$);<br>0.138 ($O_2$) | No. | 4[4] |
| $WO_3$/Tp-TAPB | 10 W LED<br>(λ>420 nm) | 1.49 ($H_2O_2$) | $O_2$ | 5[5] |
| COF-$WO_3$(TSCOFW) | 300 W Xe<br>(λ>420 nm) | 0.146 ($H_2$);<br>0.068 ($O_2$) | No. | 6[6] |
| | | 593 ($H_2$) | TEOA | |
| $WO_3$@TpPa-1-COF/rGO | 300 W Xe<br>(λ>420 nm) | 26.73 ($H_2$) | Vc | 7[7] |

| | | | | |
|---|---|---|---|---|
| $BiVO_4$-100/PCN | 300 W Xe (AM 1.5G filter) | 0.228 ($H_2$);<br>0.136 ($O_2$) | No. | 8[8] |
| CN-$WO_3$(CNWB) | 350 W Xe (λ>420 nm) | 96.4($H_2$) | TEOA | 9[9] |
| | | 0.292 ($H_2$);<br>0.132 ($O_2$) | No. | |
| $WS_2$-$WO_3\cdot H_2O$/g-$C_3N_4$ | 300 W Xe (λ≧420 nm) | 1.28 ($H_2$) | LA | 10[10] |
| ZnPtP-CP/$BiVO_4$ | 300 W Xe (λ>400 nm) | 1.1 ($H_2$);<br>0.56 ($O_2$) | No. | 11[11] |
| $MnO_x$/g-$C_3N_4$/CdS/Pt | 300 W Xe | 1.3 ($H_2$);<br>0.64 ($O_2$) | No. | 12[12] |
| | | 3.3 ($H_2$) | $Na_2S/Na_2SO_3$ | |
| 20%CdS-CTF-1 | 300 W Xe (800 nm>λ>420 nm) | 11.43 ($H_2$) | LA | 13[13] |
| $MoS_2$/TpPa-1-COF | 300 W Xe (λ>420 nm) | 5.585 ($H_2$) | Vc | 14[14] |
| TpPa-1/MIS-5 % | 300 W Xe (λ>420 nm) | 13.16 ($H_2$) | SA | 15[15] |
| 5 wt% 2D c-COFs/$WO_3$ | 415 nm LED 40 W | 80.9($H_2$) | Vc | This work |

## Section F Reference

1 S. D. Wang, L. Y. Huang, L. J. Xue, Q. Kang, L. L. Wen and K. L. Lv, *APPL CATAL B-ENVIRON.,* 2024, **358**, 124366.

2 C. Li, J. He, T. Cai, X. Chen, H. Tao, Y. Zhou and M. Zhu, *Chin. J. Catal.,* 2025, **74**, 130-143.

3 H. Ding, R. Shen, K. Huang, C. Huang, G. Liang, P. Zhang and X. Li, *Adv. Funct. Mater.,* 2024, **34**, 2400065.

4 G. Zuo, W. Chen, Z. Yin, S. Ma, Y. Wang, Q. Ji, Q. Xian, S. Yang and H. He, *Chem. Eng. J.,* 2023, **456**, 141096.

5 Y. Yang, Y. Li, X. Ma, L. Xie, D. Lv, L. Jiang, J. He, D. Chen and J. Wang, *Catal. Sci. Technol.,* 2023, **13**, 5599-5609.

6 R. Shen, G. Liang, L. Hao, P. Zhang and X. Li, *Adv. Mater.,* 2023, **35**, 2303649.

7 H. Yan, Y. H. Liu, Y. Yang, H. Y. Zhang, X. R. Liu, J. Z. Wei, L. L. Bai, Y. Wang and F.-M. Zhang, *Chem. Eng. J.,* 2022, **431**.

8 S. Sun, R. Gao, X. Liu, L. Pan, C. Shi, Z. Jiang, X. Zhang and J.-J. Zou, *Sci. Bull.,* 2022, **67**, 389-397.

9 R. Shen, L. Zhang, N. Li, Z. Lou, T. Ma, P. Zhang, Y. Li and X. Li, *ACS Catal.,* 2022, **12**, 9994-10003.

10 X. Wang, G. Hai, B. Li, Q. Luan, W. Dong and G. Wang, *Chem. Eng. J.,* 2021, **426**.

11 J. Wang, L. Xu, T. Wang, R. Li, Y. Zhang, J. Zhang and T. Peng, *Adv. Energy Mater.,* 2021, **11**.

12 J. Pan, P. Wang, P. Wang, Q. Yu, J. Wang, C. Song, Y. Zheng and C. Li, *Chem. Eng. J.,* 2021, **405**.

13 D. K. Wang, H. Zeng, X. Xiong, M. F. Wu, M. R. Xia, M. L. Xie, J. P. Zou and S. L. Luo, *Sci. Bull.,* 2020, **65**, 113-122.

14 M. Y. Gao, C. C. Li, H. L. Tang, X. J. Sun, H. Dong and F. M. Zhang, *J. Mater. Chem. A,* 2019, **7**, 20193-20200.

15 Y. Zhou, P. Dong, J. Liu, B. Zhang, B. Zhang, X. Xi and J. Zhang, *Adv. Funct. Mater.,* 2025, **35**.